INVESTIGATION OF THE ASCENT FLIGHT DYNAMICS OF THE SPACELINER CONCEPT AS A NON-SYMMETRIC LAUNCHER CONFIGURATION

S. Krummen, M. Sippel
German Aerospace Center (DLR), Institute of Space Systems, Bremen, Germany

Abstract

Determining the flight dynamic characteristics of a space transportation vehicle in its preliminary design phase is a complex task since a large variety of vehicle parameters need to be estimated. For the SpaceLiner vehicle, a concept of a hypersonic suborbital space plane, such an analysis has now been established. In this study a 6 DOF trajectory simulation has been developed to assess the general feasibility of fulfilling the mission requirements during nominal and off-nominal flight conditions.

1. NOMENCLATURE AND ABBREVIATIONS

SLV	SpaceLiner Vehicle
SLP	SpaceLiner Passenger Stage
SLB	SpaceLiner Booster Stage
SLC	SpaceLiner Capsule
SLME	SpaceLiner Main Engines
DOF	Degree of Freedom
TVC	Thrust Vector Control
LOX	Liquid Oxygen
LH2	Liquid Hydrogen
MECO	Main Engine Cut-Off
MET	Mission Elapsed Time
NED	North-East-Down Coordinate System
COG	Center of Gravity
COP	Center of Aerodynamic Pressure
COT	Center of Thrust

2. INTRODUCTION

The SpaceLiner is a concept of a hypersonic suborbital launch vehicle, which is capable of transporting 50 passengers over ultra-long-haul distances. Since 2005 this concept has been researched by the German Aerospace Center (DLR) [1], leading to the investigation of various different vehicle configurations [2].

FIG 1. Artist's impression of the SpaceLiner 7-3 during stage separation

The currently proposed baseline design, also known as *SpaceLiner 7-3*, is shown in FIG 1. As can be seen the vehicle consists of two mated stages: The passenger stage (SLP) and a booster stage (SLB) [3]. Both stages are propelled by 11 bipropellant LOX/LH2 rocket engines in total [4]. During operation the SpaceLiner Vehicle (SLV) lifts off vertically in mated configuration and climbs to an altitude of approximately 80 km. After stage separation the reusable booster stage returns to launch site while the passenger stage further accelerates to a flight-path velocity of approximately 7.2 km/s before its main engines are turned off. Henceforth the passenger stage performs a continuous gliding reentry flight to its destination, capable to cover a ground range of up to 17000 km [5]. This distance corresponds to the typical reference mission from Australia to Europe as visualized in FIG 2, which can be served by the SpaceLiner in less than 2 hours.

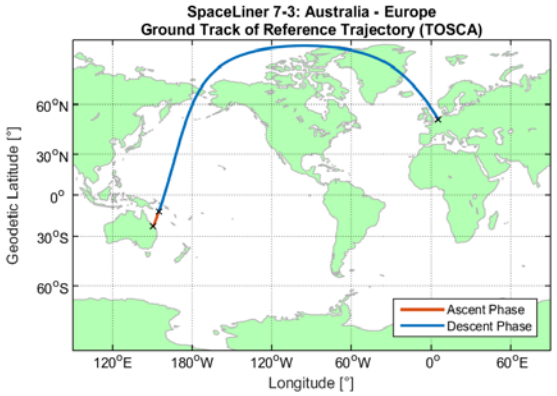

FIG 2. Ground track of the SpaceLiner reference mission from Australia to Europe

In previous system engineering studies the vehicle subsystems [6] and feasible flight trajectories [7] have already been specified. However, in these investigations the vehicle dynamics have been idealized by a point mass model, considering the translational vehicle movement only. A new study has now been established to analyze the complete rigid-body dynamics of the SpaceLiner during ascent flight in order to assess the influence of the rotational degrees of freedom on the system's feasibility [8]. This investigation is based on a flight dynamics simulation capable to determine the vehicle's state of motion in all six degrees of freedom (DOF) and a compatible SpaceLiner vehicle model. Since the SpaceLiner can be seen as a typical example for any non-

symmetrical launcher concept, the applied methods can easily be extended to similar vehicle configurations.

3. PROBLEM MODELING

For the investigation of the SpaceLiner's ascent flight dynamics a vehicle model has been developed, which extends the level of detail of previous system definitions [3]. This model has been implemented in the TRACE Simulation Framework, a DLR-internal tool based on Matlab/Simulink for simulating vehicle dynamics. The top-level structure of this simulation is sketched in FIG 3.

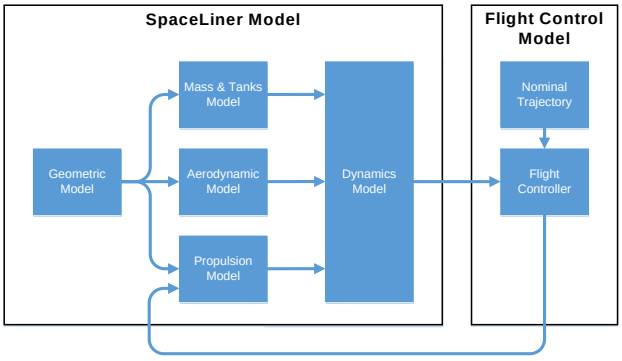

FIG 3. Top-level structure of the SpaceLiner flight dynamics simulation

Within the SpaceLiner vehicle model the non-linear time-dependent system properties are described by domain specific submodels. Furthermore a preliminary flight control model has been designed to control the thrust vector control system (TVC) during simulation.

3.1. SpaceLiner Vehicle Model

Based on the current vehicle geometry shown in FIG 4 a rigid-body model of the SpaceLiner has been developed. Transient effects are considered explicitly within this model, since the vehicle properties are subject to large variations during ascent flight.

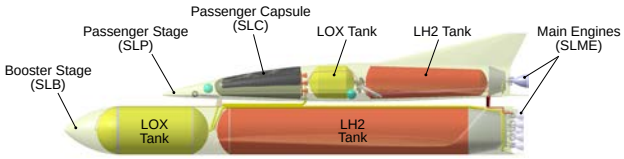

FIG 4. Overview of the SpaceLiner geometry and its major subsystems

The mass and inertia properties of the SpaceLiner are specified on subsystem level as visualized in FIG 5. For each component the properties are estimated by previous system specifications [9]. Since the majority of the SpaceLiner's inertia is generated by the loaded propellant, the subsystems model is supplemented by a tanks model which is describing the propellant distribution inside the vehicle based on the current tanks and feedline geometry [10]. The filling level of each tank is calculated dynamically during simulation in order to determine the transient inertia properties for all flight states. However, since this model describes the SpaceLiner vehicle as a rigid body, fuel sloshing and related effects are neglected.

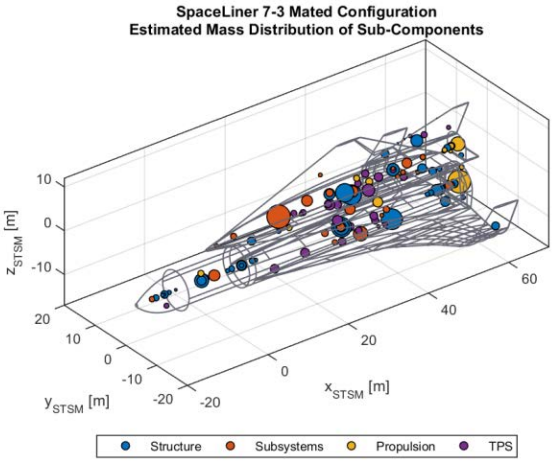

FIG 5. Mass model of the SpaceLiner subsystems; the volume of each sphere is proportional to the corresponding system masses

Besides the inertia properties also the aerodynamic characteristics of the SpaceLiner are changing significantly during ascent flight as the vehicle is passing through sub-, super- and hypersonic flow regimes with aerodynamic pressures between 0.1 – 30 kPa. In order to determine the aerodynamic coefficients of the SpaceLiner in all those flight conditions, the previously defined aerodynamic reference database has been utilized [11]. This dataset is complemented by estimations of lateral and dynamic derivatives of the aerodynamic coefficients [12].

The characteristics of the SpaceLiner Main Engines (SLME) have been determined in previous studies by simulations of the engine cycle [4] whose results are incorporated into the vehicle model. In order to provide thrust vector control during ascent flight each engine is designed to gimbal independently around its idle position. A mechanical gimbal limit of ±8° has been specified for all engines. During simulation the necessary engine deflections are determined by the flight control system.

3.2. Flight Control System

Additionally to the SpaceLiner vehicle model a preliminary flight control system has been designed to operate the TVC actuators during ascent flight. In previous investigations analyzing the translational motion of the SpaceLiner only, a simple feed-forward controller in combination with an offline optimization algorithm has been utilized [13]. However, for a 6 DOF trajectory simulation this approach is not applicable since the state variables are strongly coupled and sensitive to changes in the control variables. This issue is solved by using a closed-loop controller which is determining the control variables at simulation runtime.

A block diagram representing the top-level structure of the implemented flight control system is shown in FIG 6. As can be seen the control system adapts the classical cascade design of flight controllers for airplanes [14]. Here, the inner feedback loop is controlling the vehicle's attitude, while the outer feedback loop is providing flight-path control. The target states of the vehicle, which are

derived from a reference trajectory, are commanded to the controller.

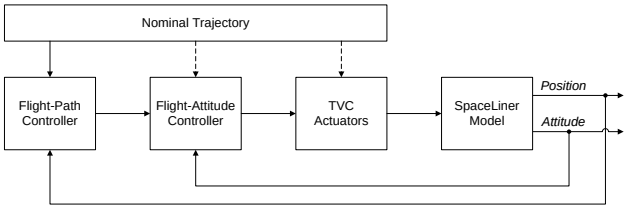

FIG 6. Cascade structure of the implemented flight control system

On the lowest level the individual deflection of each SpaceLiner Main Engine is combined to 3 control signals for attitude control which are controlled by PID feedback controllers. In particular, for pitch control all engines are deflected simultaneously in vertical direction, while yaw control is provided by equivalent lateral deflections. Roll control is executed during mated ascent by inducing an additional horizontal deflection of the passenger stage engines only. After stage separation roll control is realized by opposed vertical deflections of these two engines.

The inner feedback loop for attitude control is enclosed by the flight-path control loop which is controlling the translational deviations between a commanded trajectory and the actual position of the SpaceLiner. This control loop includes two PID controllers for vertical pitch and lateral skid-to-turn maneuvers. A lateral bank-to-turn and a throttling controller is also integrated in this level but currently not used.

In order to counteract the non-linear and transient system behavior of the SpaceLiner vehicle dynamics, the feedback gains of all PID controllers are provided by a gain-scheduling scheme based on the particular flight condition. For each operating point the feedback gains are designed by a semi-automatic relay autotuning algorithm [15, 16] utilizing empirical Ziegler-Nichols tuning rules [17]. Additionally, the trim settings for each operating point are also determined and fed forward to the TVC system to improve the follow-up behavior of the controller. Exemplary results of this algorithm for the flight-attitude control loop are plotted in FIG 7.

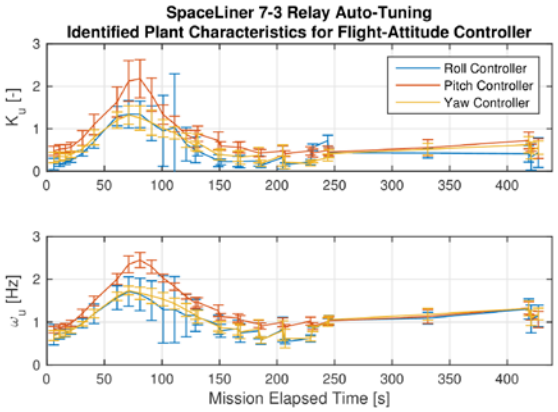

FIG 7. Identified system characteristics by the relay autotuning algorithm; Used to determine the feedback gains of the flight attitude controller

The semi-automatic design approach allows a rapid control prototyping of the flight controller during the general design process of the SpaceLiner. Even though little information about the vehicle characteristics is used by this algorithm, the resulting controller revealed sufficient quality during simulation. Nevertheless, more detailed control design procedures are currently under investigation.

4. ANALYSIS AND SIMULATION RESULTS

Based on the developed SpaceLiner vehicle model a simulation study has been concluded investigating the ascent flight dynamics on the reference mission from Australia to Europe. The major flight events for this mission are visualized in FIG 8. It should be noticed that the SpaceLiner Main Engines are sequentially cut off in upper atmospheric layers to limit the acceleration on the passengers which causes asymmetric thrust settings during periods of the ascent flight.

FIG 8. Ascent trajectory of the SpaceLiner reference mission from Australia to Europe displaying all major mission events

In the simulation study the following nominal and off-nominal cases have been analyzed:

1) Nominal undisturbed ascent trajectory
2) Ascent trajectories with atmospheric disturbances
   a) Large scale wind profiles (HWM93 [18])
   b) Moderate stochastic gusts (Karman [19])
   c) Combined disturbances (HWM93 & Karman)
3) Ascent trajectories under anomaly scenarios
   a) Reduced I_{sp} of SpaceLiner Main Engines
   b) Premature stage separation
   c) Engine failure at Lift-Off
   d) Engine failure at Max-Q

For all simulation cases predefined reference trajectories [13] are utilized as guidance command, which have been designed in previous 3 DOF simulations.

4.1. Evolution of the Vehicle Properties

As typical for all space transportation systems, the mass and inertia properties of the SpaceLiner are depending strongly on the instantaneous filling level of the propellant tanks. In particular the loaded propellant of the SpaceLiner contributes to 82% of its Gross Lift-Off Mass and forms over 99% of its principle moments of inertia. Based on the developed rigid-body model an analysis of the transient evolution of these properties has now been made possible.

The movement of the vehicle's center of gravity (COG) during ascent flight, which is caused by the continuous draining of the propellant tanks, is visualized in FIG 9. During the mated flight phase of both SpaceLiner stages, the COG is shifting 21.7 m backwards and 3.4 m upwards, which corresponds to 27% of the vehicle's length and 15% of the respective height. This significant movement needs to be considered explicitly by the flight control system in order to trim the SpaceLiner in all flight conditions.

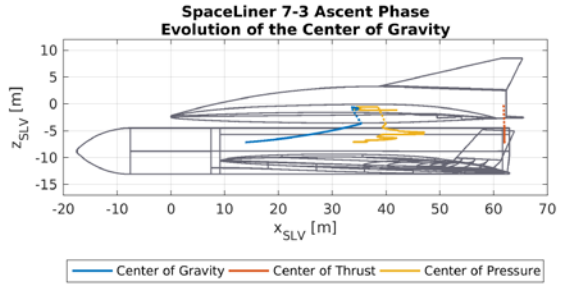

FIG 9. Transient movement of the SpaceLiner's center of gravity, center of thrust and center of aerodynamic pressure during nominal ascent flight

Furthermore, the positions of the resulting center of thrust (COT) and center of aerodynamic pressure (COP) are also changing during ascent flight. While the evolution of the COP is caused by the different aerodynamic flow regimes and the changing flight attitude, the movement of the COT arises from the sequential, asymmetric throttling of the SpaceLiner Main Engines.

4.2. Deviations to the Reference Trajectory

Since the SpaceLiner reference trajectory considers the translational motion of the vessel only, the influence of the rotational degrees of freedom on the vehicle dynamics can be estimated by comparing the simulated ascent trajectory with its reference values.

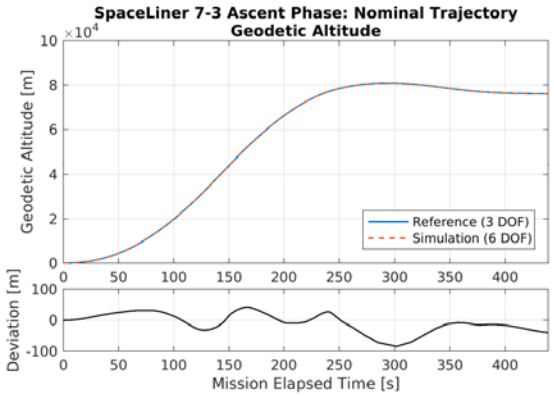

FIG 10. Simulation results for the nominal ascent trajectory; Comparison of the simulated and commanded vehicle altitude

The deviations between the commanded and the actually simulated altitude of the SpaceLiner vehicle are shown in FIG 10. As can be seen the maximum vertical displacement of the SpaceLiner with respect to the reference trajectory remains below 100 m in any flight condition. Regarding the same simulation case, the lateral displacement is limited to 60 m. Generally an additional performance loss of $\Delta v \approx -5$ m/s can be observed compared to the idealized reference trajectory. Related to the specific orbital energy of the vessel at MECO this performance reduction is less than 0.1%.

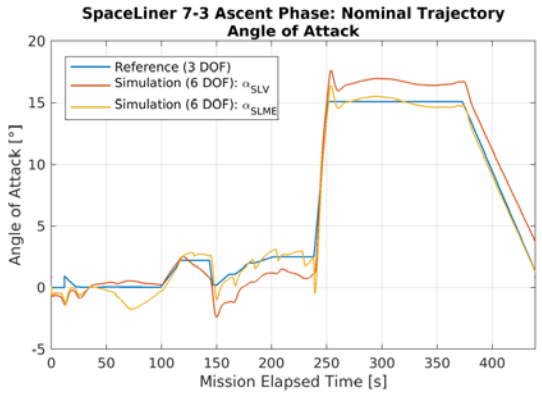

FIG 11. Simulation results for the nominal ascent trajectory; Comparison of the simulated and commanded angle of attack

Concerning the rotational motion of the SpaceLiner, FIG 11 visualizes the difference of the simulated angle of attack to its reference values. Here, the regular angle of attack with respect to the body-fixed frame α_{SLV}, as well as the angle of attack of the resulting thrust vector α_{SLME}, is displayed. For the first flight phases it can be observed that the reference values are tracked by α_{SLV} sufficiently, while in higher altitudes they are followed by α_{SLME}. This artifact is caused by the changing moment trimming mechanism in different atmospheric layers. In denser layers the aerodynamic moment needs to be trimmed by the TVC system, whereas the thrust-induced moment is the dominant force in upper layers. A similar behavior can be observed for the sideslip angle. In general it can be stated that no corrective maneuvers with excessive aerodynamic angles are executed in any simulation case, even during the sequential, asymmetric cut-off of the SpaceLiner Main Engines.

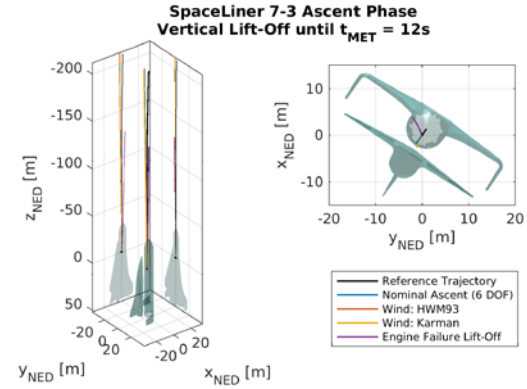

FIG 12. Flight-path deviations during the vertical lift-off phase for different simulation scenarios

The positioning accuracy of the SpaceLiner during disturbed ascent flights remains in a similar range as for the nominal case. For the general mission success these accuracies can be considered as non-critical as they are in the same order of magnitude as the vehicle's dimensions. The strictest constraints occur during take-off since a collision with the Launchpad Tower needs to be

avoided. For the considered simulation cases the flight-paths during the vertical lift-off phase are shown in FIG 12. During this first period a maximum deviation of 3.0 m from the reference path can be determined for ascent under atmospheric disturbances, as well as a deviation of 4.5 m in case of the most critical engine failure at lift-off. These margins need to be considered in the proceeding design of the launch pad.

Regarding the flight performance under off-nominal conditions an additional performance loss of $\Delta v \approx -1$ m/s compared to the nominal trajectory can be observed for moderate atmospheric disturbances, which can be covered by current system design margins. Significantly higher performance reductions have been noticed for the investigated anomaly scenarios. In case of an engine failure a reduced velocity of $\Delta v \approx -15$ m/s at MECO (-0.2% of specific orbital energy) has been observed, for a decreased I_{sp} of the SLMEs $\Delta v \approx -82$ m/s (-1.1% of specific orbital energy) and for a premature stage separation $\Delta v \approx -151$ m/s (-2.1% of specific orbital energy). Based on the current state of this study, these deficits could still be compensated by adapted descent trajectories in order to fulfil the mission. However, since these cases represent a major deviation from the nominal trajectory, further detailed investigations are necessary.

4.3. Feasibility of the TVC System

An important aspect for the dimensioning of the TVC actuators and the feasibility assessment of the control system are the maximum required TVC deflection angles during ascent flight.

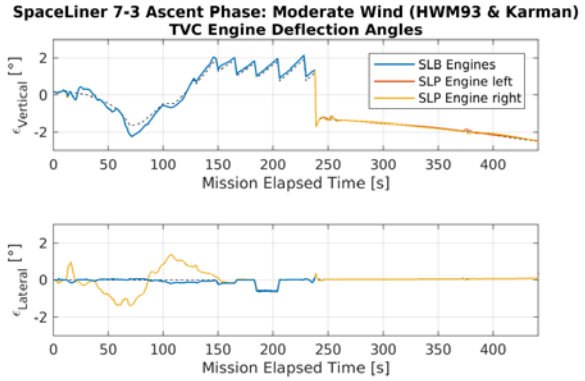

FIG 13. Lateral and vertical TVC deflections of the SpaceLiner Main Engines during ascent phase

The necessary deflections of the SpaceLiner Main Engines are shown in FIG 13 in case of a moderately disturbed atmosphere. As can be seen the maximum vertical engine deflections are limited to ±2.5° in all flight condition, while the lateral deflection angles remain below ±1.4°. Compared to the gimbal limit of ±8.5° of common liquid rocket engines [20] these deflections are considerably small. It can also be noticed that the successive throttling of the SpaceLiner engines after $t_{MET} = 150$ s effectively limits the necessary vertical deflections of the TVC actuators. The yaw moment, which is induced by this asymmetric throttling, provokes only a small lateral deflection of all engines.

Comparing the individual simulation cases it has been revealed that the engine deflections for roll control are sensitive to asymmetric loads as they occur e.g. during crosswinds. An overview of the ranges of the deflection angles for the different scenarios is given in FIG 14. While for most engines the gimbal range remains almost constant under disturbances, the lateral deflection of the SpaceLiner Passenger Stages engines, which are providing roll control during the mated ascent phase, are increasing significantly under asymmetric loads. Providing sufficient roll control can therefore be identified as a limiting factor in the design of the TVC system. However, since all engine deflections are significantly below the predefined gimbal limit of ±8°, no critical influence of the flight dynamics on the concept's feasibility can be identified based on the investigated simulation cases.

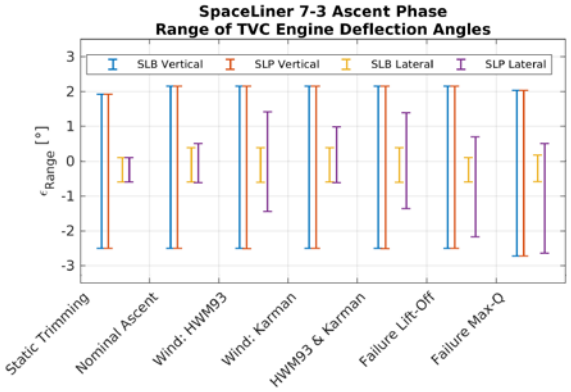

FIG 14. Ranges of the TVC deflections of the SpaceLiner Main Engines for different ascent scenarios

4.4. Trimmability and Aerodynamic Stability

A necessary condition for the controllability of the SpaceLiner during ascent flight is the ability to trim the aerodynamic moments in all flight conditions with the TVC system.

Concerning the nominal ascent trajectory FIG 15 visualizes the maximum TVC trim deflections for nominal flight conditions and variable angles of attack, and FIG 16 for variable sideslip angles respectively. Since all SpaceLiner Main Engines possess a gimbal limit of ±8° no moment trimming can be performed in the hatched flight states. Therefore at the point of maximum aerodynamic pressure the admissible flight envelope needs to be restricted to $-7° \leq \alpha_{Max\text{-}Q} \leq 4°$ and $-3° \leq \beta_{Max\text{-}Q} \leq 3°$.

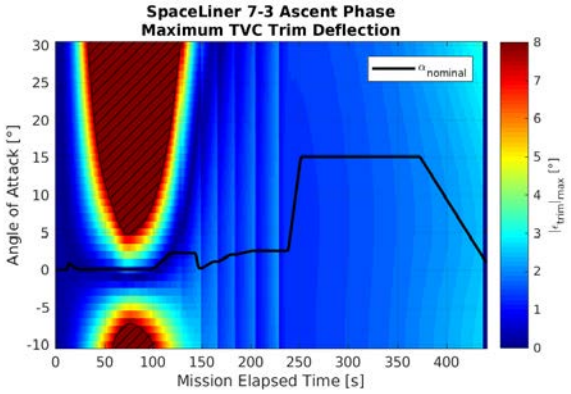

FIG 15. Maximum TVC trim deflections of the SpaceLiner Main Engines for variable angles of attack; Non-trimmable flight conditions are hatched

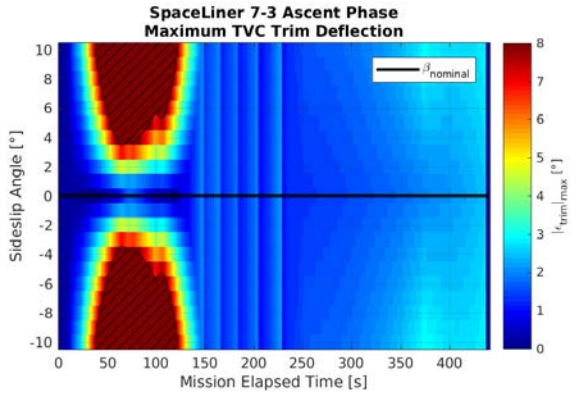

FIG 16. Maximum TVC trim deflections of the SpaceLiner Main Engines for variable sideslip angles; Non-trimmable flight conditions are hatched

Generally, the trimmability of the aerodynamic moments can be ensured for all flight conditions up to lateral aerodynamic pressures of $q\,\alpha \leq 2000$ Pa rad and $q\,\beta \leq 1500$ Pa rad. This restriction has only a marginal impact on the admissible flight envelope of the SpaceLiner since lateral aerodynamic pressures in this order of magnitude are already not desirable due to the occurring structural loads.

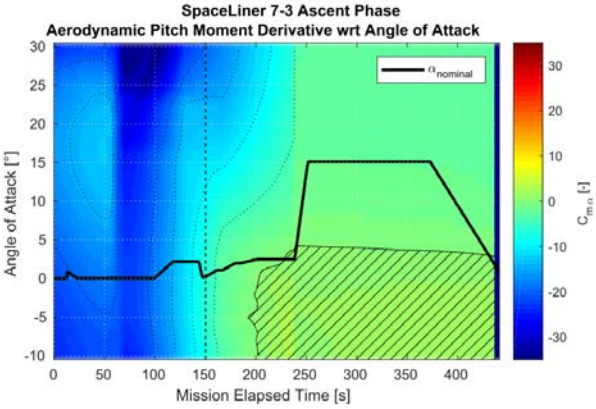

FIG 17. Longitudinal aerodynamic stability derivative $c_{m\alpha}$ for off-nominal angles of attack; Aerodynamic instable flight conditions are hatched

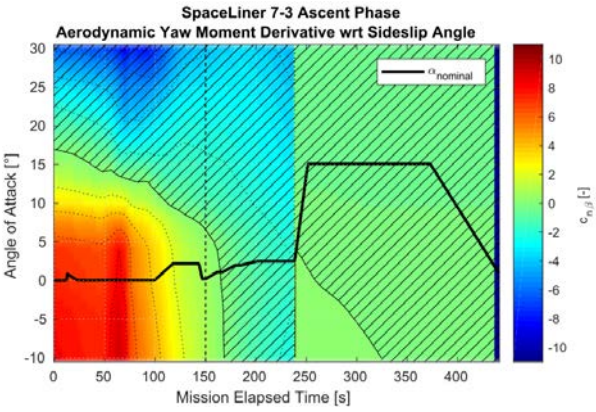

FIG 18. Lateral aerodynamic stability derivative $c_{n\beta}$ for off-nominal angles of attack; Aerodynamic instable flight conditions are hatched

Another relevant control characteristic of the SpaceLiner is the aerodynamic stability. In contrast to the trimmablility the aerodynamic stability is not a necessary condition for the general controllability of the vehicle, since the system's stability can also be provided by the flight control system. Especially in upper atmospheric layers above 50 km, where the influence of the aerodynamic pressure is almost negligible, the aerodynamic stability has practically no implications on the stability of the entire system. Nevertheless, in lower altitudes aerodynamic stable flight conditions are desirable.

The longitudinal aerodynamic stability derivative $c_{m\alpha}$ is shown in FIG 17 for a nominal ascent trajectory, and the lateral stability derivative $c_{n\beta}$ in FIG 18 respectively. In the contour plot all instable flight conditions are hatched, while a dashed line indicates the practical limit for the influence of aerodynamic effects. It should be noticed that lateral and longitudinal aerodynamic stability is given for the first flight phases except for very large angles of attack, where lateral stability could not be ensured. In higher altitudes the SpaceLiner passes through aerodynamic instable flight states, but these regimes can practically be disregarded in the assessment of the system's controllability due to the lack of sufficient aerodynamic pressure.

5. CONCLUSIONS AND OUTLOOK

Generally, regarding the vehicle's ascent flight dynamics for the investigated flight scenarios, no evidence has been found which would contradict the general feasibility of the SpaceLiner concept. The controllability of the vehicle is given for all relevant flight conditions with a sufficient positioning accuracy, while the TVC system includes acceptable design margins for off-nominal flight states. Additional performance losses, which are induced by the rotational dynamics of the SpaceLiner or atmospheric disturbances, are sufficiently small and can be covered by current system margins. Therefore the previously designed ascent trajectories of the SpaceLiner [13] appear to be feasible from a flight dynamics point of view.

In order to determine the complete admissible flight envelope of the SpaceLiner more investigations of critical mission scenarios as strongly disturbed trajectories or operational anomalies are necessary. Additionally, other flight missions need to be considered in continuative studies. More advanced tuning procedures for the flight control system are currently under investigation to optimize the resulting vehicle performance. Furthermore, more system details like structural-elastic effects and fuel sloshing should be included into future vehicle models.

6. ACKNOWLEDGEMENTS

The authors gratefully acknowledge the support of Mrs. Ingrid Dietlein and Mr. Yavor Dobrev for the realization of this study.

7. REFERENCES

[1] Sippel, M., Klevanski, J., and Steelant, J., "Comperative Study on Options for High-Speed Intercontinental Passenger Transports: Air-Breathing- vs. Rocket-Propelled" 56th International Astronautical Congress, IAC-05-D2.4.09, 2005.

[2] Sippel, M., Foreest, A., "SpaceLiner Rocket-Powered High-Speed Passenger Transportation Concept

Evolving in FAST20XX." IAC 2010, Prag, CZ, 27. Sep- 01. Oktober 2010.
[3] Sippel, M., Schwanekamp, T., Trivailo, O., Kopp, A., Bauer, C., and Garbers, N., "SpaceLiner Technical Progress and Mission Definition." 20th AIAA International Space Planes and Hypersonic Systems and Technologies Conference, AIAA 2015-3582, 06.07.2015.
[4] Sippel, M., Schwanekamp, T., Ortelt, M., "Staged Combustion Cycle Rocket Engine Subsystem Definition for Future Advanced Passenger Transport." Space Propulsion, No. 30, 2014.
[5] Sippel, M., Schwanekamp, T., Bauer, C., Garbers, N., Foreest, A. van, Tengzelius, U., Lentsch, A., "Technical Maturation of the SpaceLiner Concept" Proceedings of the 18th AIAA/3AF International Space Planes and Hypersonic Systems and Technologies Conference, AIAA 2012-5850, Tours, France, 2012.
[6] Sippel, M., Bussler, L., Kopp, A., Krummen, S., Valluchi, C., Wilken, J., Prévereaud, Y., Vérant, J.-L., Laroche, E., Sourgen, F., Bonetti, D., "Advanced Simulations of Reusable Hypersonic Rocket-Powered Stages" 21st AIAA International Space Planes and Hypersonic Systems and Technologies Conference, AIAA 2017-2170, Xiamen, March 2017.
[7] Sippel, M., Trivailo, O., Bussler, L., Lipp, S., Valluchi, C., Kaltenhäuser, S., Molina, R., "Evolution of the SpaceLiner towards a Reusable TSTO-Launcher" 67th International Astronautical Congress, IAC-16-D2.4.03, Guadalajara, September 2016.
[8] Krummen, S., "Investigation of flight dynamics and effects of rotational degrees of freedom on the flight performance of asymmetric space transportation systems based on the SpaceLiner 7 concept", SART TN-010/2016, Bremen, December 2016.
[9] Wilken, J., Bussler, L., "SpaceLiner System Specification Document", SL-SS-SART-00026-1/0, Bremen, August 2017.
[10] Schwanekamp, T., Ludwig, C., Sippel, M., "Cryogenic Propellant Tank and Feedline Design Studies in the Framework of the CHATT Project" 19th AIAA International Space Planes and Hypersonic Systems and Technologies conference, AIAA Aviation and Astronautics Forum and Exposition, June 2014
[11] Schwanekamp, T., Morsa, L., Zuppardi, G., Molina, R., "SpaceLiner 7-2 Aerodynamic Reference Database", SART TN-026/2012, Bremen, 2012.
[12] Rosema, C., Doyle, J., Auman, L., Underwood, M., Blake, W., "Missle Datcom: User's Manual – 2011 Revision", Air Force Research Laboratory, AFRL-RB-WP-TR-2011-3071, 2011.
[13] Casali, E., Bussler, L., Sippel, M., "Investigation of feasible flight trajectories and re-entry atmospheric guidance for SpaceLiner 7", SART TN-014/2015, 2015.
[14] Brockhaus, R., Alles, W., Luckner, R., "Flugregelung", 3rd edn., Springer, 2011.
[15] Aström, K., Hägglund, T., "Automatic Tuning of Simple Regulators with Specification on Phase and Amplitude Margins", Automatica, Vol. 20, No. 5, 1984, pp. 645-651
[16] Yu, C.-C., "Autotuning of PID Controllers. A Relay Feedback Approach", 2nd edn., Springer, 2006.
[17] Wilson, D. I., "Relay-based PID tuning." Automation and Control, Vol. 2005, pp. 10–11
[18] Hedin, A.E., Fleming, E.L., Manson, A.H., Scmidlin, F.J., Avery, S.K., Clark, R.R., Franke, S.J., Fraser, G.J., Tsunda, T., Vial, F., Vincent, R.A., "Empirical Wind Model for the Upper, Middle and Lower Atmosphere", Journal of Atmospheric and Terrestrial Physics, Vol. 58, No. 13, pp. 1421-1447, 1996.
[19] U.S. Department of Defense, "Flying Qualities of Piloted Aircraft", MIL-HDBK-1797, December 1997.
[20] Dumoulin, J. "NSTS 1988 News Reference Manual, http://science.ksc.nasa.gov/shuttle/technology/sts-newsref/stsref-toc.html#sts-mps", [retrieved 20 August 2017].